Electrochemical Kinetics of Ag|Ag+ and TMPD|TMPD+• in the Room−Temperature Ionic Liquid [C4mpyrr][NTf2]; toward Optimizing Reference Electrodes for Voltammetry in RTILs

ARTICLE *in* THE JOURNAL OF PHYSICAL CHEMISTRY C · AUGUST 2007

Impact Factor: 4.77 · DOI: 10.1021/jp0737754

8 AUTHORS, INCLUDING:

Debbie S. Silvester
Curtin University
55 PUBLICATIONS **1,670** CITATIONS
SEE PROFILE

Leigh Aldous
University of New South Wales
89 PUBLICATIONS **1,827** CITATIONS
SEE PROFILE

Electrochemical Kinetics of $Ag|Ag^+$ and $TMPD|TMPD^{+\bullet}$ in the Room-Temperature Ionic Liquid $[C_4mpyrr][NTf_2]$; toward Optimizing Reference Electrodes for Voltammetry in RTILs

Emma I. Rogers,[†] Debbie S. Silvester,[†] Sarah E. Ward Jones,[†] Leigh Aldous,[‡] Christopher Hardacre,[‡] Angela J. Russell,[§] Stephen G. Davies,[§] and Richard G. Compton*,[†]

Physical and Theoretical Chemistry Laboratory, University of Oxford, South Parks Road, Oxford OX1 3QZ, United Kingdom, School of Chemistry and Chemical Engineering/QUILL, Queen's University Belfast, Belfast, Northern Ireland BT9 5AG, United Kingdom, and Department of Organic Chemistry, University of Oxford, Chemistry Research Laboratory, Mansfield Road, Oxford, OX1 3TA, United Kingdom

Received: May 16, 2007; In Final Form: July 23, 2007

The voltammetry and kinetics of the $Ag|Ag^+$ system (commonly used as a reference electrode material in both protic/aprotic and RTIL solvents) was studied in the room-temperature ionic liquid *N*-butyl-*N*-methylpyrrolidinium bis(trifluoromethylsulfonyl)imide, $[C_4mpyrr][NTf_2]$ on a 10 μm diameter Pt electrode. For the three silver salts investigated (AgOTf, $AgNTf_2$, and $AgNO_3$, where OTf^- = trifluoromethanesulfonate, NTf_2^- = bis(trifluoromethylsulfonyl)imide, and NO_3^- = nitrate), the voltammetry gave rise to a redox couple characteristic of a "deposition/stripping" process at the platinum electrode surface. Using potential step chronoamperometry, the diffusion coefficients of AgOTf, $AgNTf_2$, and $AgNO_3$ were found to be 1.05, 1.17, and 5.00×10^{-11} m^2 s^{-1}. All three voltammograms were theoretically modeled to reveal surprisingly slow standard electrochemical rate constants, k^0, of 2.0, 1.5, and 0.19×10^{-4} cm s^{-1} respectively for the $Ag^+|Ag^0$ couple. As a potentially faster alternative to the $Ag|Ag^+$ system, the voltammetry and kinetics of the $TMPD|TMPD^{+\bullet}$ system (where TMPD = *N*,*N*,*N*′,*N*′-tetramethyl-*p*-phenylenediamine) was also studied, using neutral TMPD and two TMPD radical cation salts, with BF_4^- and NTf_2^- counter anions. Diffusion coefficients for TMPD, $TMPD^{+\bullet}BF_4^-$, and $TMPD^{+\bullet}NTf_2^-$ were calculated to be 1.84, 1.35, and 1.43×10^{-11} m^2 s^{-1} respectively, and a k^0 value of $2.6-2.8 \times 10^{-3}$ cm s^{-1} was obtained from theoretical fitting of the cyclic voltammetry. This number is an order of magnitude larger than that for the $Ag|Ag^+$ system, allowing for the suggestion that the $TMPD|TMPD^{+\bullet}$ system may be more suitable than the $Ag|Ag^+$ system as a redox couple for use in reference electrodes for ionic liquids.

1. Introduction

Room-temperature ionic liquids (RTIL) are characterized as salts that exist in the liquid state around 298 K.[1,2] They are comprised of a bulky, asymmetric organic cation and a weakly coordinating inorganic (sometimes organic) anion; the combination of which determines the properties of the solvent. Ionic liquids possess several properties including high electrical conductivity, low vapor pressure (low-volatility), low combustibility, high chemical and thermal stability, and favorable solvating properties.[1−4] In recent years, ionic liquids have attracted increasing interest because of their low-volatility and hence are greener for the environment compared with volatile organic compounds (VOCs).[2] They have been employed in a wide range of electrochemical applications[1−3,5] and have experimental advantages over conventional solvents because of their intrinsic conductivity and wide electrochemical windows.[1−4] They are also 1−2 orders of magnitude more viscous than conventional solvents such as acetonitrile and water, and the diffusion coefficients of electroactive species are accordingly lowered.[1,2]

The search for suitable reference electrodes for use in ionic liquid media is currently active[6] and has been reviewed recently.[7] In protic and aprotic solvents however, there have been many reference electrode systems used, described in detail by Butler[8] and Ives and Janz.[9] The hydrogen electrode has been adopted universally in water and water-based solvents, and all other reference electrodes are measured relative to this. Other examples of reference electrodes used in aqueous solvents include the aqueous calomel electrode (quite common) and electrodes based on chlorine and silver−silver chloride.[8,9] There are also a range of reference electrode systems used in aprotic solvents (MeCN, DMF, and DMSO) such as alkali metals (e.g., $Li|Li^+$), thallium ($Tl|Tl^+$), cadmium ($Cd|Cd^{2+}$), and zinc ($Zn|Zn^{2+}$), as well as mercury ($Hg|Hg^{2+}$) as an internal standard.[8] Often, for simplicity, a platinum or silver wire is used as a quasi-reference (or pseudoreference) electrode in nonaqueous solvents, and it has become standard practice to use a quasi-reference electrode in combination with an electrochemically reversible couple.[4,5,10] International Union of Pure and Applied Chemistry (IUPAC) recommend the use of ferrocene/ferrocenium (Cp_2Fe/Cp_2Fe^+)[11] or cobaltocenium/cobaltocene (Cp_2Co^+/Cp_2Co)[4] as stable redox couples with respect to shifts in potential.

In respect to nonhaloaluminate ionic liquids, Bond et al.[4] have used the cobaltocene/cobaltocenium couple in the RTIL 1-butyl-

* Author to whom all correspondence should be addressed. E-mail: richard.compton@chemistry.oxford.ac.uk. Phone: +44 (0) 1865 275 413. Fax: +44 (0) 1865 275 410.
† Physical and Theoretical Chemistry Laboratory.
‡ Queen's University Belfast.
§ Department of Organic Chemistry.

10.1021/jp0737754 CCC: $37.00
Published on Web 08/28/2007

3-methylimidazolium hexafluorophosphate, [C_4mim][PF_6]. Saheb et al.[5] report the use of a silver wire immersed in both $Ag|Ag^+$ (0.1 M $AgNO_3$) and Ag|AgCl (0.1 M Bu_4NCl) in the ionic liquids 1-butyl-3-methylimidazolium tetrafluoroborate, [C_4mim][BF_4], 1-butyl-3-methylimidazolium bis(trifluoromethylsulfonyl)imide, [C_4mim][NTf_2], and [C_4mim][PF_6]. Snook et al.[12] evaluate the $Ag|Ag^+$ couple as a reference in RTILs, using silver trifluoromethanesulfonate, AgTf, a silver triflate salt (we will use the nomenclature AgOTf in this report) as an alternative to $AgNO_3$ in *N*-butyl-*N*-methylpyrrolidinium bis(trifluoromethylsulfonyl)imide, [C_4mpyrr][NTf_2], and test the stability of the reference system in a number of common RTILs.

At present, the electrode kinetics of the $Ag|Ag^+$ couple has not been studied in detail in ionic liquids, even though the couple is widely advocated and employed as a reference electrode. However, this is fundamental in deciding whether a reference system may be suitable in RTIL media. Electrode kinetic studies on the $Cp_2Fe|Cp_2Fe^+$ system in the RTIL 1-ethyl-3-methylimidazolium bis(trifluoromethylsulfonyl)imide, [C_2mim][NTf_2], have been previously shown to be relatively fast, with a standard electrochemical rate constant of 0.21 cm s^{-1}.[13] The aim of the work undertaken in this study is therefore to evaluate the use of three silver salts in the RTIL, [C_4mpyrr][NTf_2], AgOTf (as suggested by Snook et al.),[12] $AgNTf_2$ (with same anion as the RTIL), and $AgNO_3$ (used in aprotic solvents and in a few RTIL studies) and to compare them to the kinetics of the $Cp_2Fe|Cp_2Fe^+$ couple. We will also suggest the possibility of using a reference system based on TMPD|$TMPD^{+\bullet}$ (*N*,*N*,*N*′,*N*′-tetramethyl-*p*-phenylenediamine and its radical cation) by studying the kinetics of neutral TMPD and two of its salts, $TMPD^{+\bullet}BF_4^-$ (tetrafluoroborate) and $TMPD^{+\bullet}NTf_2^-$ (bis(trifluoromethylsulfonyl)imide), as an alternative to $Ag|Ag^+$.

2. Experimental Section

2.1. Chemical Reagents. [C_4mpyrr][NTf_2] was prepared in house following standard procedures reported in literature.[14] Ferrocene (Aldrich, 98%), tetrabutylammonium perchlorate (TBAP, Fluka, Puriss electrochemical grade, >99%), acetonitrile (Fischer scientific, dried and distilled, >99%), silver nitrate ($AgNO_3$, BDH Chemicals), silver triflate (AgOTf, Aldrich, 99.95+%), and *N*,*N*,*N*′,*N*′-tetramethyl-*p*-phenylenediamine (TMPD, Fluka, >98%) were used as received, without further purification.

Silver bis(trifluoromethylsulfonyl) imide, ($AgNTf_2$) was synthesized as follows. $AgNO_3$ (4.1 g, 0.024 mol) was dissolved in 80 mL deionized water. To this a solution of NaOH (1.4 g, 0.036 mol) in 60 mL deionized water was added under stirring. This was stirred for 10 min, and the dark brown precipitate was collected by vacuum filtration. The precipitate was washed with ultrapure water until the washings were pH neutral and then was added to a solution of $HNTf_2$ (7.0 g, 0.025 mol) in 100 mL deionized water. This was stirred for 30 min, and the white precipitate was collected by vacuum filtration and washed until pH neutral, yielding $AgNTf_2$ (6.2 g, 0.016 mol, 67%).

Samples of $TMPD^{+\bullet}$ radical cation salts were prepared following modified procedures based on Michaelis and Granick's method.[15] $TMPD^{+\bullet}BF_4^-$ was prepared following the method described by Yamauchi et al.[16] TMPD (500 mg, 3.04 mmol) was dissolved in a solution of MeOH (12 mL) and H_2O (9 mL) containing $NaBF_4$ (4.49 g, 40.9 mmol). The solution was cooled to −10 °C and a 0.252 M solution of Br_2 (15.7 mL, 3.95 mmol, 1.3 eq) was added dropwise with vigorous stirring. The resulting precipitate was isolated by filtration and washed with cold MeOH followed by dry Et_2O. The crude product was recrystallized from MeOH to furnish $TMPD^{+\bullet}BF_4^-$ (280 mg, 1.11 mmol, 37%) as a purple solid with a melting point T_m = 120−121 °C (dec) [literature[16] T_m = 126−127 °C (MeOH, dec)].

$TMPD^{+\bullet}NTf_2^-$ was prepared according to a modified version of the procedure described above. TMPD (100 mg, 0.608 mmol) was dissolved in MeOH (2.4 mL) and H_2O (1.8 mL). The solution was cooled to −20 °C and lithium bis(trifluoromethylsulfonyl)imide (2.35 g, 8.18 mmol) was added in one portion. The resulting solution was degassed, and a 0.252 M solution of Br_2 (2.41 mL, 0.608 mmol, 1.0 eq) was added dropwise at −20 °C under nitrogen with vigorous stirring. The resulting precipitate was isolated by filtration under a stream of nitrogen gas, and washed with cold H_2O followed by dry Et_2O. The crude product was recrystallized from degassed MeOH/H_2O under nitrogen to furnish $TMPD^{+\bullet}NTf_2^-$ (128 mg, 47%) as a dark purple solid with a melting point T_m = 109−110 °C (dec).

2.2. Instrumentation. A computer controlled μ-Autolab potentiostat (Eco-Chemie, Netherlands) was used to perform electrochemical experiments. For the silver solutions, a three-electrode arrangement was employed, with a platinum microelectrode (10 μm diameter) as the working electrode, a Ag/Ag^+ as the reference electrode, and a platinum wire as the counter (auxiliary) electrode. The reference electrode consisted of a silver wire immersed in a glass tube containing 10 mM Ag^+ in [C_4mim][NO_3], separated from the bulk solution with a Vycor frit. Solutions of Ag^+ in [C_4mpyrr][NTf_2] were made up directly into the 1.5 mL ionic liquid to approximately 100 mM concentrations (0.8 mM $AgNO_3$ because of low solubility). All solutions were sealed in foil-covered cells, stirred, and purged under vacuum on the Schlenk line for several hours prior to use. The cells consisted of glass vials topped with a 15 mm thick PTFE cylinder containing four holes, into which the three electrodes and a nitrogen line was placed. The solutions were purged throughout experiment by passing nitrogen through the sealed cell.

For the neutral TMPD and TMPD salt solutions, a conventional two-electrode arrangement was employed with a Pt working electrode (10 μm diameter) and a silver wire quasi-reference electrode (0.5 mm diameter).[17] The electrodes were housed in a "T cell"[18] specifically designed for studying microsamples of ionic liquids under a controlled atmosphere. A small section of a disposable pipet tip was used to modify the microelectrode and create a small cavity above the surface into which 20 μL of sample was placed. The cell was covered in foil and kept in the dark inside a closed Faraday cage, which also served to minimize background noise. TMPD (7.5 mM), $TMPD^{+\bullet}BF_4^-$ (2 mM), and $TMPD^{+\bullet}NTf_2^-$ (1 mM) were made up directly in 1 mL of RTIL which was additionally purged under vacuum (0.05 Torr) for 2 h.

The microdisk electrode was polished using alumina of size 1 μm and 0.3 μm (Kemet Ltd., U.K.) on soft lapping pads (Beuhler, Illinois) and was calibrated by analyzing the steady-state voltammetry of 2 mM ferrocene in acetonitrile with 0.1 M TBAP, adopting a value for the diffusion coefficient of 2.3×10^{-9} m^2 s^{-1}.[19]

2.3. Chronoamperometric Experiments. Chronoamperometric transients were achieved using a sample time of 0.01 s. The solution was held at 0 V for 20 s (pretreatment), after which the potential was stepped to a position after the peak, and the current was measured for 10 s. The experimental data was fit using the software package Origin 7.0 (Microcal Software Inc.) using a nonlinear curve fitting function which follows the Shoup and Szabo[20] fitting function as employed by Evans et al.[21] The

equations used in this approximation are given below and are sufficient to describe the current response within an accuracy of 0.6%.

$$I = -4nFDcr_d f(\tau) \quad (1)$$

$$f(\tau) = 0.7854 + 0.8863\tau^{-1/2} + 0.2146e^{-0.7823\tau^{-1/2}} \quad (2)$$

$$\tau = \frac{4Dt}{r_d^2} \quad (3)$$

where n is the number of electrons transferred, F is the Faraday constant, D is the diffusion coefficient, c is the initial concentration, r_d is the radius of the electrode, and t is the time. The value for the radius of the electrode was fixed, and 100 iterations were performed by the software to give a value for the diffusion coefficient, D, and a product of the number of electrons multiplied by concentration, nc. Note that the measurement of D in this manner ascribes a value to a Fickian diffusion coefficient; nothing is implied about the exact chemical identity of the electrochemical species. In particular, Ag^+ might, for example, very likely be complexed with anions from the RTIL.

3. Theory

The following mathematical model was designed to extract electrode kinetic data for the deposition of Ag^+ from solution and the stripping of silver (Ag) from silver on the electrode from experimental data. The model will be used to investigate the kinetics of the $Ag|Ag^+$ couple proposed as the basis of reference electrodes in RTILs.

3.1 Mathematical Model. A "thick layer" coverage of silver on a microdisk electrode of radius r_d is considered allowing the rate of dissolution of Ag from the surface is be modeled as independent of the position dependent coverage of silver, Γ_{Ag} surface coverage. This avoids the complicated system of mixed kinetics between the reaction of Ag on Ag and Ag on the Pt electrode. For simulation purposes, the height of the silver deposit formed on the electrode was approximated as zero so that the microdisk can be modeled as a flat disk.

The $Ag|Ag^+$ couple is assumed to follow a simple one-electron transfer using Butler−Volmer kinetics.

$$Ag^+(sol) + e^- \rightleftharpoons Ag(s) \quad (4)$$

k_f and k_b are the deposition and stripping rate constants defined by:

$$k_f = k^0 \exp\left(\frac{-\alpha F}{RT}(E - E_f^0)\right) \quad (5)$$

$$k_b = k^0[Ag^+]^0 \exp\left(\frac{(1-\alpha)F}{RT}(E - E_f^0)\right) \quad (6)$$

where k^0 is the surface process rate constant in centimeter per second for the $Ag^+|Ag$ couple, α is the transfer coefficient, and E_f^0 is the formal potential. $[Ag^+]^0$ is the standard concentration equal to 1×10^{-3} mol cm^{-3}. R is the ideal gas constant (8.314 J K^{-1} mol^{-1}), F is the Faraday constant (96485 C mol^{-1}), and T is the temperature (298 K).

Figure 2 in Supporting Information shows the coordinate system used. Because of this system having cylindrical symmetry, only a two-dimensional simulation in one plane is needed. The mass transport of Ag^+ in solution to and from the electrode surface is defined according to Fick's first law by the following equation:

$$\frac{\partial[Ag^+]}{\partial t} = D\left(\frac{\partial^2[Ag^+]}{\partial r^2} + \frac{1}{r}\frac{\partial[Ag^+]}{\partial r} + \frac{\partial^2[Ag^+]}{\partial z^2}\right) \quad (7)$$

where D is the diffusion coefficient of Ag^+ in $[C_4mpyrr][NTf_2]$. The change in the position dependent surface coverage of silver, Γ_{Ag}, with time is described by the following equation:

$$\frac{\partial\Gamma_{Ag}}{\partial t} = k_f[Ag^+]_{surf} - k_b \quad (8)$$

Γ_{Ag} is not permitted to go below zero as zero represents the point where all silver has been stripped from that part of the electrode. To apply this condition in the model, k_b is set equal to zero once $\Gamma_{Ag} = 0$ is reached. If for any time step, dt, d$\Gamma_{Ag} > -k_b\,dt + k_f[A]_{Z=0}\,dt$, then the value k_b is adjusted so that $k_b\,dt = -d\Gamma_{Ag} + k_f[A]_{Z=0}\,dt$.

At the beginning of the electrochemical experiment, the platinum microdisk has a clean surface free from any silver deposits, and the only silver present is in the form of Ag^+ ions in the bulk solution. The initial mathematical conditions ($t = 0$) are therefore:

$$[Ag^+] = [Ag]_{bulk} \quad \text{for} \quad 0 \le r \le r_{max} \quad \text{and} \quad 0 \le z \le z_{max}$$

$$\Gamma_{Ag} = 0 \quad \text{for} \quad 0 \le r \le r_d \quad \text{and} \quad z = 0$$

where r_{max} and z_{max} represent the size of the simulation space in the r and z direction, respectively. These parameters take the value of $6\sqrt{Dt}$ and represent a semi-infinite distance in the system.

During the experiment ($t > 0$) the diffusion of Ag^+ in solution is subject to boundary conditions, which represent the nonflux boundaries and the bulk concentration of Ag^+ condition at the semi-infinite boundaries. The following equations represent these boundary conditions for $t > 0$:

$$[Ag^+] = [Ag]_{bulk} \quad \text{for} \quad 0 \le r \le r_{max} \quad \text{and} \quad z = z_{max}$$

$$[Ag^+] = [Ag]_{bulk} \quad \text{for} \quad r = r_{max} \quad \text{and} \quad 0 \le z \le z_{max}$$

$$\frac{\partial[Ag^+]}{\partial r} = 0 \quad \text{for} \quad r = 0 \quad \text{and} \quad 0 \le z \le z_{max}$$

$$\frac{\partial[Ag^+]}{\partial r} = 0 \quad \text{for} \quad r_d \le r \le r_{max} \quad \text{and} \quad z = 0$$

At the disc surface ($0 \le r \le r_d$, $z = 0$), the following condition applies:

$$D\frac{\partial[Ag^+]}{\partial z} = \frac{\partial\Gamma_{Ag}}{\partial t} = k_f[Ag^+]_{z=0} - k_b \quad (9)$$

The current can be calculated using the following equation:

$$I = -2\pi F\int_0^{r_d}\frac{\partial\Gamma_{Ag}}{\partial t}r\,dr \quad (10)$$

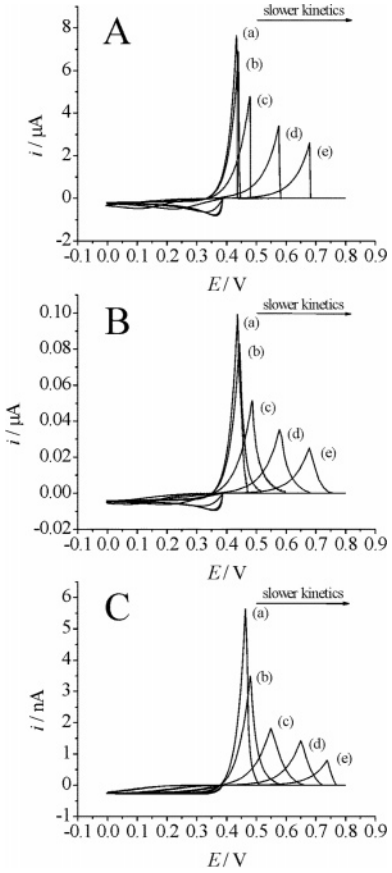

Figure 1. Simulated voltammograms for different size electrodes and rate constants. $\alpha = 0.5$, $E_f^0 = 0.45$ V, $D = 8 \times 10^{-12}$ m^2 s^{-1}, $[c]_{bulk} = 84$ mM, and $\upsilon = 100$ mV s^{-1}. The electrode radius, r_d, is (A) 100 μm, (B) 10 μm, and (C) 1 μm and the rate constant, k^0, is (a) 1×10^{-2} cm s^{-1}, (b) 1×10^{-3} cm s^{-1}, (c) 1×10^{-4} cm s^{-1}, (d) 1×10^{-5} cm s^{-1}, and (e) 1×10^{-6} cm s^{-1}.

3.2. Numerical Simulation and Convergence. The system of partial differential equations was solved using a fully implicit finite difference scheme[22] combined with Newton's method[23] and using an extended version of the Thomas algorithm.[24] The simulation space was covered with an expanding grid[25] that expands exponentially from the electrode/inert material boundary and the electrode surface. The convergence of the simulation program was tested to ensure a convergence error of less than 1% when compared with over-converged simulations. The program was written for Delphi 7 and run on a personal computer.

The initial deposition of silver on the platinum microdisk in the experimental cyclical voltammetry (CV) is controlled by nucleation processes and is not covered by this model. The kinetic data to be extracted from the experiment is all contained within the reverse scan and this allows the need for simulation of the nucleation process to be avoided. When simulating the reverse scan, it is necessary to approximate the electrode coverage and solution concentration profile so that they represent the conditions in the system for the start of the reverse scan. This was done by running the simulation as a linear sweep starting at a potential that is more negative than the switching potential of the CV. The start potential of the linear sweep was chosen so that the charge passed during the deposition phase was approximately equal to the charge passed during the stripping phase.

3.3. Simulated Voltammograms. Figure 1shows the result of simulations run to examine the effect of different values of the rate constant, k^0, and electrode radius, r_d, on the stripping peak. These scans were run as CVs.

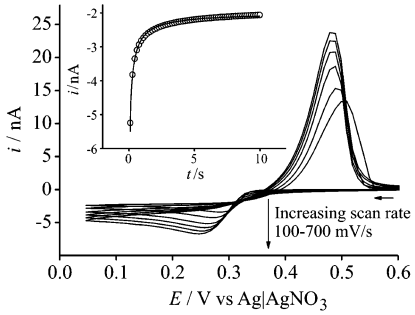

Figure 2. CV for the reduction of 85 mM AgOTf in [C_4mpyrr][NTf_2] on a platinum microelectrode (diameter 10 μm) at varying scan rates (100, 200, 300, 400, 500, and 700 mV s^{-1}). Inset is the experimental (solid line) and fitted theoretical (dots) chronoamperometric transients recorded for the reduction of AgOTf. The potential was stepped from +0.5 to 0.1 V.

For all electrode radii, faster kinetics result in a narrower peak that occurs at a lower potential. The drop of the right-hand side of the peak becomes sharper as the potential range, over which the metal at different points on the electrode runs out, is smaller because of the faster stripping kinetics.

On the larger electrode ($r_d = 100$ μm), planar diffusion occurs over most of the surface and results in a sharp drop on the right-hand side of the peak as the metal runs out at all points of the electrode surface at approximately the same time. On smaller electrodes, hemispherical diffusion results in a greater build up of metal near the electrode edge than in the center, which means that the drop in the current is spread over a wider potential as the metal runs out at different times at different points on the electrode surface. The differences between the simulation and the experimental results caused by various approximations used will be discussed in section 4.1.2.

4. Results and Discussion

The ionic liquid [C_4mpyrr][NTf_2] (see Figure 1, Supporting information) was chosen as the solvent throughout this work because it had a wide electrochemical window (ca. 5 V) which showed no residual features after the RTIL was placed under vacuum. Another reason for choosing this particular RTIL was to evaluate the viability of using AgOTf as a reference electrode material in this RTIL, as previously suggested by Snook et al.[12] Therein, a reference electrode incorporating a silver wire immersed in 10 or 100 mM AgOTf in [C_4mpyrr][NTf_2] was devised. The $Ag|Ag^+$ couple was then evaluated using the ferrocene and cobaltocenium hexafluorophosphate redox couples, and the potential was found to be stable to within 1 mV over a period of three weeks when 10 mM AgOTf was used.[12]

The aim of the work reported here is to voltammetrically characterize the $Ag|Ag^+$ redox couple by studying the voltammetry of AgOTf in an RTIL solution. This is compared with two other silver salts, $AgNTf_2$ and $AgNO_3$, and the $TMPD|TMPD^+$ couple as alternatives to AgOTf. In the latter case, we explore two different $TMPD^{+\bullet}$ salts, $TMPD^{+\bullet}BF_4$ and $TMPD^{+\bullet}NTf_2$.

4.1. Electrochemical Reduction of AgOTf in [C_4mpyrr][NTf_2]. *4.1.1. Experimental Results.* Figure 2shows cyclic voltammetry for the reduction of 85 mM AgOTf (OTf = $CF_3SO_3^-$) in [C_4mpyrr][NTf_2] on a 10 μm platinum microelectrode at scan rates from 100 to 700 mV s^{-1}. The voltammetry is reported against a silver/silver nitrate reference electrode, which consists of a silver wire immersed in 10 mM $AgNO_3$ in the RTIL [C_4mim][NO_3],[26] and has been used in two previous

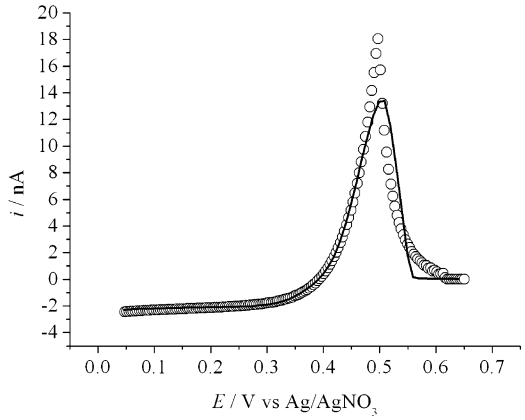

Figure 3. Experimental (solid line) and fitted simulation (dots) data for the reverse scan for the reduction of 85 mM AgOTf in [C_4mpyrr][NTf_2] on a platinum microelectrode (diameter 10 μm) at a scan rate of 100 mV s^{-1}.

studies from our laboratory.[27,28] The voltammetry gives rise to a broad reduction peak at +0.29 V versus Ag|$AgNO_3$ (at 100 mV s^{-1}) and a corresponding sharp oxidation peak at +0.50 V versus Ag|$AgNO_3$ (at 100 mV s^{-1}). The peaks are characteristic of a "deposition/stripping" process and are similar to those observed by He et al.[29] for the electrochemical deposition of silver on a glassy carbon electrode in [C_4mim][PF_6] and [C_4mim][BF_4]. Normally, steady state behavior is expected on a microelectrode of such small diameter. However, because of the high viscosity of RTILs, diffusion is much slower, giving rise to peak shaped voltammetry.[30] A plot of peak current versus square root scan rate was found to be linear for the reductive peak. The peak separation increases with scan rate, consistent with a quasi-reversible electrochemical system.

In the present study, it is believed that silver is first deposited onto the platinum surface, followed by formation of bulk silver, which is then "stripped off" on the anodic scan. The deposition/stripping is further supported by the observation of a crossover of the oxidative and reductive sweeps of the cyclic voltammogram. This crossed area of the scan, often called a "nucleation loop", is characteristic of a nucleation process occurring at the electrode surface.[29] Both the presence of the loop and the absence of underpotential[31] suggests that deposition of silver onto platinum is less thermodynamically favorable than deposition onto silver.

In order to calculate a diffusion coefficient for AgOTf in [C_4mpyrr][NTf_2], a potential step was performed on the reductive part of the wave. The potential was stepped from +0.5 V to a potential after the reduction peak. The resulting chronoamperometric transient is shown inset to Figure 2 (solid line) along with a theoretical fit to the Shoup and Szabo[20] equation (dots). The electron count was calculated to be 1, and the diffusion coefficient was 1.05 ($\pm$0.10) $\times$ 10^{-11} m^2 s^{-1}.

4.1.2. Simulation Results. In order to gain kinetic information about the Ag|AgOTf couple, the mathematical model described in section 3 was used to simulate the reverse scan of the experimental data obtained for an 85 mM AgOTf solution at a scan rate of 100 mV s^{-1}. Figure 3 shows the best fit for the experimental data (solid line) with the simulation data (dots), and the parameters used are summarized in Table 1. In this case, the diffusion coefficient obtained (1.05×10^{-11} m^2 s^{-1}) from the simulation of AgOTf in [C_4mpyrr][NTf_2] is consistent with that obtained by chronoamperometry. The rate constant, k^0, obtained for the Ag|AgOTf couple was 2.0 ($\pm$0.05) $\times$ 10^{-4} cm s^{-1} which is considered slow for an ideal reference electrode.

It can be seen from Figure 3 that the left-hand side of the stripping peak obtained from the simulation fits the experimental data well, and from this part of the scan, all of the parameters given in Table 1 can be extracted. The shape of the right-hand side of the peak is largely determined by the distribution of the coverage of silver deposited on the electrode as a drop in current occurs when there is no silver remaining on the electrode surface. The small difference between the top and the right-hand side of the peak obtained from simulation and that obtained via experiment is due to differences in the build up of silver coverage, which mainly occurs on the forward scan of the CV.

TABLE 1: Parameters for Ag Stripping from AgOTf, $AgNTf_2$, and $AgNO_3$ from the Simulation Fits Shown in Figure 3 (Main Text), and Figures 3 and 4 (Supporting Information) Where In All Cases $\alpha = 0.5$

compound	concn, mM	scan rate, mV s^{-1}	D, m^2 s^{-1}	E^0 versus Ag/$AgNO_3$, V	k^0, cm s^{-1}
AgOTf	84.7	100	1.05×10^{-11}	+0.475	2.0×10^{-4}
$AgNTf_2$	102.0	100	5.60×10^{-12}	+0.470	1.5×10^{-4}
$AgNO_3$	0.8	20	5.00×10^{-11}	+0.460	1.9×10^{-5}

The model predicts that more silver is deposited near the electrode edge because of the hemispherical nature of the diffusion that produces the "edge effect" associated with microdisk electrodes. This has been observed to be true for the deposition of copper on boron-doped diamond microdisk arrays[32] and is expected to be the case for silver deposition. From this distribution, it is predicted that the silver depletes initially in the center of the electrode with the silver depleting at the electrode edge last and, in doing so, determines that shape of the right-hand side of the peak.

Because of the absence of a full model that takes the nucleation process into account, the complete forward scan cannot be modeled accurately, and as such, the coverage distribution in the simulation is only approximate. In addition, the current at the edge of a microdisk electrode is, in theory, infinite leading to a very large coverage buildup at the electrode edge. In reality, the coverage cannot become as high as predicted as a deposit so tall in relation to the deposit in the center of the electrode would be unstable in solution. This creates an experimental stripping peak where the current drops off much faster than predicted by the simulation. This is likely to be the biggest cause of the difference between the shapes of the simulation and experimental data. Nevertheless, the method is capable of extracting electrode kinetic data to a satisfactory level of accuracy and precision. In particular, for the purpose of evaluating rate constants as related to reference electrodes, it is the order of magnitude (1, 0.1, 10^{-2}, 10^{-3} cm s^{-1}, ...) which is pertinent.

The kinetic information obtained is for the stripping of silver from silver. Toward the end of the stripping process, silver is also being stripped off of the platinum electrode. This problem will apply for all of the cases when this model is used in this paper, and it is more prominent when there is only a small amount of silver deposited on the electrode. The remaining parameters are discussed in section 4.9.

4.2. Electrochemical Reduction of $AgNTf_2$ in [C_4mpyrr][NTf_2]. *4.2.1. Experimental Results.* Cyclic voltammetry for the reduction of 102 mM $AgNTf_2$ on a 10 μm diameter platinum electrode at scan rates from 100 to 700 mV s^{-1} is shown in Figure 4. As observed for AgOTf (Figure 2), a reduction and oxidation peak characteristic of deposition/stripping is observed. In Figure 4, the reduction peak at +0.26 V versus Ag|$AgNO_3$ (100 mV s^{-1}) corresponds to the deposition of silver onto Pt, and the oxidation peak at +0.51 V (100 mV s^{-1}) is the

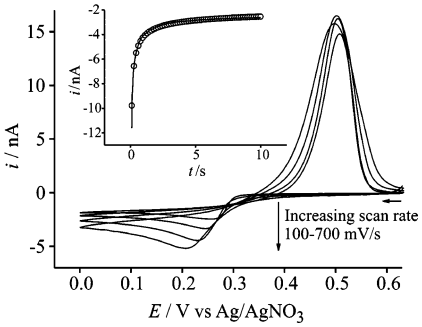

Figure 4. CV for the reduction of 102 mM $AgNTf_2$ in [C_4mpyrr][NTf_2] on a platinum microelectrode (diameter 10 μm) at varying scan rates (100, 200, 400, and 700 mV s^{-1}). Inset is the experimental (solid line) and fitted theoretical (dots) chronoamperometric transients recorded for the reduction of $AgNTf_2$. The potential was stepped from +0.5 to 0.1 V.

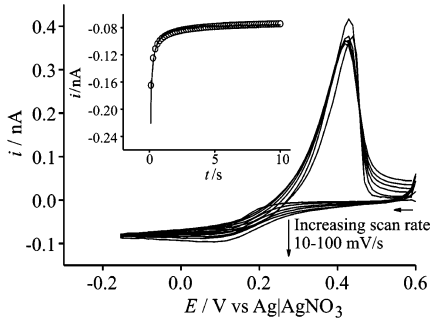

Figure 5. CV for the reduction of 0.8 mM $AgNO_3$ in [C_4mpyrr][NTf_2] on a platinum microelectrode (diameter 10 μm) at varying scan rate (10, 20, 40, 70, and 100 mV s^{-1}). Inset is the experimental (solid line) and fitted theoretical (dots) chronoamperometric transients recorded for the reduction of $AgNO_3$. The potential was stepped from +0.5 to −0.15 V.

dissolution or "stripping" of the deposited silver. Here, the nucleation loop is more obvious for $AgNTf_2$ (Figure 4) than for AgOTf (Figure 2), which also supports the suggestion that deposition of silver onto platinum is less thermodynamically favorable than deposition of silver onto silver. A plot of peak current versus square root scan rate was found to be linear for the deposition peak. The peak separation increases with scan rate, again like AgOTf, consistent with a quasi-reversible electrochemical system.

The inset to Figure 4 shows the experimental (solid line) and fitted theoretical (dots) chronoamperometric transients for the reduction of $AgNTf_2$ in [C_4mpyrr][NTf_2] on a Pt electrode (d = 10 μm). The potential was stepped from +0.5 to 0.0 V. Theoretical fitting of the experimental transient to the Shoup and Szabo[20] equation revealed an electron count of 1 and a diffusion coefficient of 1.17 (±0.10) × 10^{-11} m^2 s^{-1}, comparable to that of AgOTf (see above).

4.2.2. Simulation Results. To obtain kinetic information about the Ag|$AgNTf_2$ couple, the mathematical model described in section 3 was used to simulate the experimental data obtained for a 102 mM $AgNTf_2$ solution at a scan rate of 100 mV s^{-1} in the same way as for the AgOTf (section 4.1.2). Figure 3 in Supporting Information shows the best fit of the experimental data (solid line) with the simulation (dots), and the parameters used are summarized in Table 1. In this case, the diffusion coefficient obtained from the simulation for $AgNTf_2$ in [C_4mpyrr][NTf_2] is lower than that obtained by chronoamperometry. The rate constant, k^0, was found to be 1.5 × 10^{-4} cm s^{-1}, which is of the same order of magnitude as that for AgOTf. The remaining parameters are discussed in section 4.9.

4.3. Electrochemical Reduction of $AgNO_3$ in [C_4mpyrr][NTf_2]. To move further toward the understanding of the kinetics of silver salts in ionic liquids, silver nitrate was studied. $AgNO_3$ has been employed previously as a reference electrode by both Silvester et al.[28] in [C_4mpyrr][NTf_2] and Aldous et al.[27] in [C_4mim][NTf_2]. However, the stability of this reference couple in ionic liquids has not yet been fully investigated. Here, we report the experimental and simulated voltammetry of $AgNO_3$ in [C_4mpyrr][NTf_2].

4.3.1. Experimental Results. Figure 5 shows a cyclic voltammogram for the reduction of 0.8 mM $AgNO_3$ in [C_4mpyrr][NTf_2] on a platinum microelectrode (diameter 10 μm) at scan rates of 10 to 100 mV s^{-1}. A broad reductive peak is observed at +0.08 V versus Ag|$AgNO_3$ (100 mV s^{-1}), with a corresponding oxidation peak at approximately +0.42 V (100 mV s^{-1}). A plot of peak current versus square root scan rate was linear for the reductive peak.

A potential step was performed on the reductive wave, and the resulting chronoamperometric transient is shown in the inset of Figure 5 (solid line). From theoretical fitting of the experimental data to the Shoup and Szabo[20] expression (dots), an electron count of 1 was obtained, with a diffusion coefficient of 5.0 (±0.5) × 10^{-11} m^2 s^{-1}, comparable in magnitude to that of AgOTf and $AgNTf_2$ (see above) and approximately 1−2 orders of magnitude less than that obtained in conventional solvents (1.7 × 10^{-9} m^2 s^{-1} in water,[33] 2.9 × 10^{-10} m^2 s^{-1} in dimethyl sulfoxide (DMSO)),[34] because of the higher viscosity of the RTIL (80 cP for [C_4mpyrr][NTf_2][35] versus 1.00 cP for H_2O and 1.99 cP for DMSO at 298 K).

4.3.2. Simulation Results. Kinetic information for the Ag|$AgNO_3$ couple was obtained using the same method as for AgOTf and $AgNTf_2$, fitting the experimental data for a 0.8 mM $AgNO_3$ solution at a scan rate of 20 mV s^{-1}. $AgNO_3$ is not very soluble in [C_4mpyrr][NTf_2], so a lower concentration solution was used for this experiment as the mathematical model does not take the saturation limit of the compound into account. This low concentration causes a problem as only a thin layer of Ag is deposited on the electrode, and the model is designed to look at Ag on Ag deposition rather than a mixture of processes with silver depositing on the Pt microdisk as well as on its self. To help reduce this problem, data from a 20 mV s^{-1} scan rate was simulated as this allowed for a thicker layer of silver to be deposited. Figure 4 in Supporting Information shows the best fit of the experimental (solid line) with the simulation (dots), and the parameters used are summarized in Table 1. Here, the diffusion coefficient obtained from the simulation for $AgNO_3$ in [C_4mpyrr][NTf_2] is consistent with that from chronoamperometry. The rate constant, k^0, was found to be 1.9 × 10^{-5} cm s^{-1} which is slower than for AgOTf and $AgNTf_2$.

4.4. Theoretical Results for Reference Electrodes Based on Stripping Voltammetry. During experiments, a small current is passed by the reference electrode and potentiostat and is usually quoted as the input bias current. Typical values range from 5 × 10^{-12} to 5 × 10^{-11} A.[36] The effect of this current, i_{ref}, can be explored for the case of reference electrodes based on stripping voltammetry using the model described in section 3. When examining the reverse scan of the CV, a potential range, ΔE, can be defined as the difference in potential between where the current is $+i_{ref}$ and when it is $-i_{ref}$. The magnitude of ΔE gives an indication of the error introduced by the current i_{ref}, when using the redox couple under study as a reference electrode. Table 2 shows the potential range, E, for a range of electrode radii, r_d, rate constants, k^0, and reference electrode currents, i_{ref}.

TABLE 2: Potential Range, ΔE, for Different Reference Electrode Currents, i_{ref} of a Range of Sizes of Electrodes Possessing Different Kinetics: $\alpha = 0.5$, $E_f^0 = 0.45$ V, $D = 8 \times 10^{-12}$ m^2 s^{-1}, $[c]_{bulk} = 84$ mM, and $v = 100$ mV s^{-1}

	1	ΔE/V			
disk radius/μm	k^0/cm s^{-1}	$i_{ref} = 5 \times 10^{-12}$ A	$i_{ref} = 5 \times 10^{-11}$ A	$i_{ref} = 5 \times 10^{-10}$ A	$i_{ref} = 5 \times 10^{-9}$ A
1	1×10^{-2}	1.3×10^{-3}	1.4×10^{-2}		
	1×10^{-3}	1.6×10^{-3}	1.8×10^{-2}		
	1×10^{-4}	4.4×10^{-3}	4.6×10^{-2}		
10	1×10^{-2}	6.8×10^{-5}	6.8×10^{-4}	7.1×10^{-3}	
	1×10^{-3}	7.4×10^{-5}	7.4×10^{-4}	7.6×10^{-3}	
	1×10^{-4}	1.3×10^{-4}	1.3×10^{-3}	1.3×10^{-2}	
100	1×10^{-2}	1.7×10^{-6}	1.7×10^{-5}	1.7×10^{-4}	1.7×10^{-3}
	1×10^{-3}	1.8×10^{-6}	1.8×10^{-5}	1.8×10^{-4}	1.8×10^{-3}
	1×10^{-4}	2.4×10^{-6}	2.4×10^{-5}	2.4×10^{-4}	2.4×10^{-3}

The data in Table 2 shows that for larger electrodes the current drawn from the reference electrode has a small ΔE value. However, at small electrodes, especially with slow kinetics, the value of ΔE is greatly increased. Larger values for ΔE are associated with greater inaccuracy in the experiment being caused by the current passed by the reference electrode. Large electrodes and fast kinetics are therefore best for reference electrodes as they reduce the effect of i_{ref} on the experiment. Examination of Table 2 shows that the use of large Ag wires is desirable for reference electrodes constructed using the Ag|Ag$^+$ couple to avoid errors resulting from the relatively slow electrode kinetics of this couple. That said, provided this caveat is followed, the couple is likely to serve as a satisfactory reference electrode unless the potentiostat used draws an unusually high current.

4.5. Electrochemical Oxidation of TMPD in [C$_4$mpyrr][NTf$_2$]. As an alternative to silver salts, the electrochemistry of TMPD was next studied. TMPD is known[30,37] to give two oxidative reversible redox couples, which may have faster electrochemical kinetics than the silver salts. Cyclic voltammetry for the oxidation of 7.5 mM TMPD in [C$_4$mpyrr][NTf$_2$] on a platinum microdisk electrode (diameter 10 μm) at 100 mV s^{-1} is shown in Figure 6a. The voltammetry shows two well-defined reversible oxidation waves (at +0.25 V and +0.85 V vs Ag respectively), which have been assigned in previous studies[30,37] to the formation of the radical cation, TMPD$^{+\bullet}$ (first step), and the dication, TMPD^{2+} (second step), following eqs 11 and 12. The peak separations for both redox couples decrease with increasing scan rate, indicating that the reactions are electrochemically reversible, and a plot of peak current versus square root scan rate for all peaks is linear, suggesting that the processes are diffusion controlled.

$$\mathrm{TMPD} \rightleftharpoons \mathrm{TMPD}^{+\bullet} + \mathrm{e}^- \quad (11)$$

$$\mathrm{TMPD}^{+\bullet} \rightleftharpoons \mathrm{TMPD}^{2+} + \mathrm{e}^- \quad (12)$$

In order to calculate the diffusion coefficient of TMPD in [C$_4$mpyrr][NTf$_2$], and to confirm the concentration, a potential step was performed on the solution. The potential was stepped from −0.25 V to a potential value after the first oxidative wave. The resulting chronoamperometric transient is shown in the inset to Figure 6a (solid line), with the theoretical fit to the Shoup and Szabo[20] expression shown as dots. Assuming an electron count of 1, the concentration was accurate to within 10% (8.1 ± 0.8 mM), and the diffusion coefficient for TMPD in [C$_4$mpyrr][NTf$_2$] was calculated to be 1.84 (±0.1) × 10^{-11} m^2 s^{-1}, comparable in magnitude to values of D obtained by Evans et al.[37] (0.57, 1.28, and 4.08 × 10^{-11} m^2 s^{-1} for TMPD in [P$_{14666}$][NTf$_2$], [C$_{10}$mim][NTf$_2$], and [C$_2$mim][NTf$_2$], respectively). Using a viscosity of 80 cP for [C$_4$mpyrr][NTf$_2$],[35] the value of D reported in this work fits well to a straight-line plot of diffusion coefficient versus the inverse of viscosity and is therefore consistent with the previous study.[37]

The kinetics of the first wave (eq 11) will be reported using digital simulation in section 4.7 (see later) and will be compared to that obtained for the three silver salts. First, in order for a stable reference system, a source of neutral TMPD and a TMPD cation species must exist together in solution, and last long enough for use in electrochemical experiments. The voltammetry of TMPD$^{+\bullet}$ with a [BF$_4$]$^-$ anion has previously been reported in a range of RTILs[37] and was used to calculate diffusion coefficients for the radical cation and dication. However, there was no mention of the stability of TMPD$^{+\bullet}$BF$_4^-$ either in air or in solution or of the reproducibility of the voltammetry. Here, we report the voltammetry of TMPD$^{+\bullet}$BF$_4^-$ and a second source of the radical cation; a new compound with an NTf$_2^-$ anion, which matches the anion used in the RTIL in this study. Sections 4.5 and 4.6 show the voltammetry of the two compounds, TMPD$^{+\bullet}$BF$_4^-$ and TMPD$^{+\bullet}$NTf$_2^-$, in [C$_4$mpyrr][NTf$_2$], which is followed by Section 4.7, which shows the kinetic analysis of the neutral TMPD and the two TMPD salts using digital simulation.

4.6. Electrochemical Reduction of TMPD$^{+\bullet}$BF$_4^-$ in [C$_4$mpyrr][NTf$_2$]. The reduction of 2 mM TMPD$^{+\bullet}$BF$_4^-$ in [C$_4$mpyrr][NTf$_2$] on a 10 μm diameter platinum microelectrode at 100 mV s^{-1} is shown in Figure 6b. Two redox couples are observed, as with TMPD, which correspond to eqs 11 and 12. However, as the TMPD exists as the radical cation, the peak potentials are shifted by approximately 0.30 V in the cathodic direction, as the radical cation is now easier to oxidize. The radical cation, TMPD$^{+\bullet}$, is reduced to the neutral species at a potential of −0.15 V versus Ag, with reoxidation back to the radical cation at −0.01 V. Oxidation of the radical cation produces the dication at a potential of +0.58 V versus Ag, which is re-reduced at +0.44 V. A plot of peak current versus square root scan rate was linear, suggesting that the processes are diffusion controlled. The stability of the compound in the RTIL of choice was evaluated from the size and shapes of the voltammetric peaks; a noticeable change in the peak height over an extended period of time (but not on the voltammetric time scale) suggests that the radical cation is unstable. Studying the compound over a period of time indicated that the compound is stable, when dissolved in the ionic liquid, for approximately 5 days.

Potential step chronoamperometry was performed on a platinum microelectrode ($d = 10$ μm) in order to calculate the diffusion coefficient for TMPD$^{+\bullet}$BF$_4^-$ in [C$_4$mpyrr][NTf$_2$]. The potential was stepped from +0.2 to −0.38 V, and the current was measured for 10 s. The resulting transient is shown as an inset to Figure 6b, with the experimental data shown as a solid

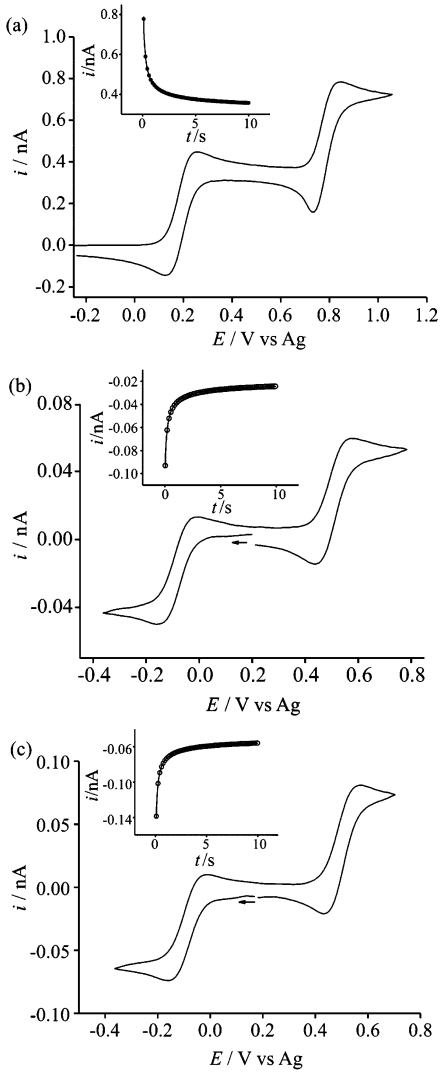

Figure 6. CV for (a) the oxidation of 7.5 mM TMPD, (b) the reduction of 2 mM $TMPD^{+\bullet}BF_4^-$, and (c) the reduction of 1 mM $TMPD^{+\bullet}NTf_2^-$ in [C_4mpyrr][NTf_2] on a platinum microelectrode (diameter 10 μm) at 100 mV s^{-1}. Insets to all figures are the experimental (solid line) and fitted theoretical (dots) chronoamperometric transients recorded for the oxidation of TMPD to $TMPD^{+\bullet}$. The potential was stepped from (a) −0.25 to +0.45 V, (b) +0.2 to −0.38 V, and (c) +0.2 to −0.35 V.

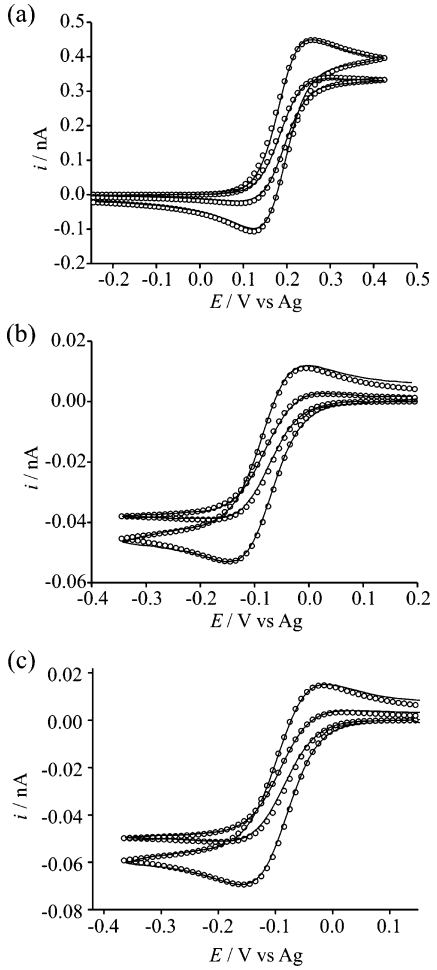

Figure 7. Comparison of experimental (line) and simulation (○) cyclic voltammograms for the reduction of (a) 7.5 mM TMPD, (b) 2 mM $TMPD^{+\bullet}BF_4^-$, and (c) 1 mM $TMPD^{+\bullet}NTf_2^-$ in [C_4mpyrr][NTf_2] at scan rates of 10 and 100 mV s^{-1}, using values of D and c close to that obtained from chronoamperometric data. Parameters are given in Table 3.

line and the theoretical fit to the Shoup and Szabo[20] expression shown as dots. The diffusion coefficient obtained for $TMPD^{+\bullet}BF_4^-$ was 1.35 (±0.15) × 10^{-11} m^2 s^{-1}, which (as with TMPD above) fits well to a straight line plot of D against 1/viscosity, using the values calculated from a previous study,[37] as expected for Stokes−Einstein behavior. The reduction peak will be simulated (in section 4.8) to obtain various kinetic parameters, which will allow us to determine the suitability of TMPD and its salt as reference materials in room-temperature ionic liquids.

4.7. Electrochemical Reduction of $TMPD^{+\bullet}NTf_2^-$ in [C_4mpyrr][NTf_2]. Figure 6c shows the reduction of 1 mM $TMPD^{+\bullet}NTf_2^-$ in [C_4mpyrr][NTf_2] on a 10 μm diameter platinum microelectrode at a scan rate of 100 mV s^{-1}. As with neutral TMPD and $TMPD^{+\bullet}BF_4^-$, two redox couples are observed, which correspond to eqs 11 and 12. The reduction of the TMPD radical cation to the neutral species occurs at −0.16 V versus Ag, with reoxidation back to the radical cation at −0.01 V. The potential of oxidation of the radical cation to the dication occurs at +0.57 V versus Ag, and the re-reduction occurs at +0.44 V. A plot of peak current against square root scan rate is linear for all peaks, indicating that the processes are under diffusion control. The shapes of the voltammetric peaks were stable for approximately 7 days when the compound was dissolved in the RTIL. However, a noticeable change in the peak heights was observed over a long period of time (but not on the voltammetric time scale), indicating that the TMPD radical cation species is unstable, even when dissolved in a RTIL with the same anion.

A potential step was performed on the reductive wave in order to calculate a diffusion coefficient of the TMPD radical cation. The potential was stepped from +0.2 to −0.35 V, and the current was measured for 10 s. The resulting chronoamperometric transient is shown in the inset of Figure 6c (solid line) with the theoretical fit to the Shoup and Szabo[20] expression (dots). A diffusion coefficient for $TMPD^{+\bullet}NTf_2^-$ of 1.43 (±0.12) × 10^{-11} m^2 s^{-1} was obtained, similar to that calculated for $TMPD^{+\bullet}BF_4^-$ and smaller than that of the neutral species (1.84 × 10^{-11} m^2 s^{-1}), which is not unexpected since the radical cation is a charged species and will move more slowly. The voltammetry of the reduction peak of $TMPD^{+\bullet}NTf_2^-$ will be simulated in the next section to obtain several kinetic parameters. This will indicate whether TMPD and its salt might be suitable reference electrode materials in RTIL media.

4.8. Simulating the Voltammetry of TMPD, $TMPD^{+\bullet}BF_4^-$, and $TMPD^{+\bullet}NTf_2^-$ in [C_4mpyrr][NTf_2]. Although the voltammetry appears electrochemically reversible, a detailed kinetic analysis is required to determine whether the TMPD|$TMPD^{+\bullet}$ system has faster kinetics than the $Ag|Ag^+$ couple. Since the

TABLE 3: Parameters for TMPD, $TMPD^{+\bullet}BF_4^-$, and $TMPD^{+\bullet}NTf_2^-$ from the Simulation Fits Shown in Figure 7 Where In All Cases $\alpha = 0.5$

compound	concn/mM	scan rate/mV s^{-1}	$D_{TMPD}/m^2\ s^{-1}$	$D_{TMPD+\bullet}/m^2\ s^{-1}$	E^0 vs Ag/V	k^0/cm s^{-1}
TMPD	7.5	10−1000	1.80×10^{-11}	1.45×10^{-11}	+0.180	2.8×10^{-3}
$TMPD^{+\cdot}BF_4^-$	2.0	10−1000	1.80×10^{-11}	1.45×10^{-11}	−0.076	2.6×10^{-3}
$TMPD^{+\cdot}NTf_2^-$	1.0	10−1000	1.78×10^{-11}	1.45×10^{-11}	−0.087	2.8×10^{-3}

TABLE 4: Summary of the Peak Potentials (vs Ag) for TMPD and Cc Redox Couples in Several Room-Temperature Ionic Liquids

RTIL	$E_{p(ox)}$ TMPD/V	$E_{p(red)}$ TMPD/V	$E_{1/2}$/V	$E_{p(red)}$ Cc/V	$E_{p(ox)}$ Cc/V	$E_{1/2}$/V	ΔE_{pp}/V
$[C_2mim][NTf_2]$	+0.239	+0.094	+0.167	−0.984	−0.834	−0.909	1.076
$[C_4mim][NTf_2]$	+0.564	+0.432	+0.498	−0.636	−0.505	−0.571	1.069
$[C_4mpyrr][NTf_2]$	+0.246	+0.125	+0.186	−0.958	−0.846	−0.902	1.088
$[N_{6,2,2,2}][NTf_2]$	+0.297	+0.186	+0.242	−0.903	−0.771	−0.837	1.079
$[C_4mim][BF_4]$	+0.228	+0.103	+0.166	−0.996	−0.857	−0.927	1.093
$[C_4mim][PF_6]$	+0.236	+0.129	+0.183	−0.962	−0.855	−0.909	1.092

standard electrochemical rate constant, k^0, calculated for Ag^+ in AgOTf, $AgNTf_2$, and $AgNO_3$ was 2.0, 1.5, and 0.19×10^{-4} cm s^{-1}, respectively, the k^0 value must be larger than 2.0×10^{-4} cm s^{-1} for the TMPD|$TMPD^+$ system to be more suitable as a redox couple for reference electrodes in RTILs.

The first oxidation wave for TMPD and first reductive wave for $TMPD^{+\bullet}BF_4^-$ and $TMPD^{+\bullet}NTf_2^-$ (eq 11) was simulated using the one-dimensional simulation program available in DigiSim 3.03 (BAS Technicol).[38] A simple one-electron mechanism was entered following eq 11, and the kinetic parameters were adjusted to give the best fit over a range of scan rates (10−1000 mV s^{-1}). According to the following inequality:[30,39]

$$\upsilon \ll \frac{RTD}{nFr_d^2} \tag{13}$$

where υ is the scan rate, R is the universal gas constant, and T is the absolute temperature, assuming $D = 1.8 \times 10^{-11}$ m^2 s^{-1} for TMPD and 1.45×10^{-11} m^2 s^{-1} for $TMPD^{+\bullet}$ and $r = 5.13$ μm; true steady state behavior can only be achieved at scan rates much less than 17.6 mV s^{-1} for TMPD and 14.1 mV s^{-1} for $TMPD^{+\bullet}$. Since the simulation is run over the range of 10 to 1000 mV s^{-1}, planar diffusion is expected to apply for this system, allowing for simulation using one-dimensional diffusion.[30,40] Figure 7 shows the best theoretical fit (dots) to the cyclic voltammograms obtained on a 10 μm diameter Pt electrode (solid line) for (a) TMPD, (b) $TMPD^{+\bullet}BF_4^-$, and (c) $TMPD^{+\bullet}NTf_2^-$ in $[C_4mpyrr][NTf_2]$ at scan rates of 10 and 100 mV s^{-1}. All three compounds were successfully simulated, and the kinetic parameters obtained from the best fit are given in Table 3. The simulations fit well to the experimental data for all three species using very similar values of the diffusion coefficients of neutral TMPD and its radical cation and using similar values of the heterogeneous rate constant, k^0. The diffusion coefficients agree well with those obtained from chronoamperometry (sections 4.5, 4.6, and 4.7), suggesting that this is a model system. The value for the heterogeneous rate constant was found to be between 2.6 and 2.8×10^{-3} cm s^{-1}, approximately ten times larger than that calculated for any of the silver salts investigated (Table 1).

4.9. Comparison of All Results. The results from theoretical fitting to the voltammetry of the six species studied (AgOTf, $AgNTf_2$, $AgNO_3$, TMPD, $TMPD^{+\bullet}BF_4^-$, and $TMPD^{+\bullet}NTf_2^-$) indicate that the heterogeneous electrochemical rate constant, k^0, is approximately 1 order of magnitude smaller for the silver salts (2.0, 1.5, and 0.19×10^{-4} cm s^{-1} for AgOTf, $AgNTf_2$, and $AgNO_3$, respectively) than for TMPD and its radical cation ($2.6-2.8 \times 10^{-3}$ cm s^{-1}). These results suggest that the $Ag|Ag^+$ system shows quite slow kinetics for a reference electrode. This suggests that the TMPD|$TMPD^{+\bullet}$ system may be more suitable than $Ag|Ag^+$ as a reference electrode material inside RTILs, provided a stable source of the TMPD radical cation can be obtained. However, both redox couples are believed to have much slower kinetics than the $Cp_2Fe|Cp_2Fe^+$ system, which was shown to have a k^0 value of 0.21 cm s^{-1} in $[C_2mim][NTf_2]$.[13] Although the different nature of the RTIL used here may influence this value slightly, it is not expected to change over an order of magnitude and will probably still be much larger than that for TMPD ($2.6-2.8 \times 10^{-3}$ cm s^{-1}).

If TMPD is to be incorporated into a reference electrode, it is useful to know the potential of the TMPD|$TMPD^{+\bullet}$ couple relative to a known redox couple, for example, ferrocene/ferrocenium (Fc/Fc^+) or cobaltocene/cobaltocenium (Cc/Cc^+), and to know if this potential varies when the RTIL is changed. Although the potentials of the Fc/Fc^+ and Cc/Cc^+ couples are not expected to vary when the anion/cation nature is changed, it is not known if the potential of the TMPD|$TMPD^{+\bullet}$ couple is constant. To investigate this, the voltammetry of both TMPD and cobaltocenium hexafluorophosphate in solution was investigated in six different RTILs with a range of common cations and anions, namely, $[C_4mpyrr][NTf_2]$, $[C_2mim][NTf_2]$, $[C_4mim][NTf_2]$, hexyltriethylammonium bis(trifluoromethylsulfonyl)-imide ($[N_{6,2,2,2}][NTf_2]$), $[C_4mim][BF_4]$, and $[C_4mim][PF_6]$. In all six ionic liquids studied, the two characteristic oxidative redox couples for TMPD oxidation were observed at positive potentials, and two characteristic reductive redox couples for $CcPF_6$ were observed at negative potentials (voltammetry not shown). The peak potentials and half wave potentials for the first TMPD oxidation and first $CcPF_6$ reduction are reported in Table 4. It can be seen that the potential of TMPD oxidation relative to cobaltocenium reduction does not vary significantly (maximum 24 mV) when the cation or anion of the RTIL is varied, suggesting that TMPD|$TMPD^{+\bullet}$ may indeed have the ability to be used as a stable redox couple in most RTIL media.

5. Conclusions

The investigation into the electrochemical kinetics of the $Ag|Ag^+$ system in the room-temperature ionic liquid $[C_4mpyrr][NTf_2]$ has revealed a relatively slow electrochemical rate constant for the $Ag|Ag^+$ system (of the order $\times 10^{-4}$ cm s^{-1}). This is approximately 1 order of magnitude slower than that calculated for the TMPD|$TMPD^{+\bullet}$ redox couple ($2.6-2.8 \times 10^{-3}$ cm s^{-1}), allowing the suggestion that TMPD and its radical cation salt may be a more suitable redox couple than $Ag|Ag^+$ for use as reference electrode material in room-temperature ionic liquids. However, the availability and stability of the TMPD

radical cation salt may hinder the widespread use of this couple in reference electrode systems, which ideally should be stable for long periods of time.

Acknowledgment. E.I.R. thanks the EPSRC; D.S.S. thanks Schlumberger Cambridge Research; S.E.W.J. thanks NERC, and L.A. thanks the Department of Education and Learning in Northern Ireland and Merck GmBH for financial support.

Supporting Information Available: Figures showing the structure of the ionic liquid, a three-dimensional representation of the cylindrical coordinate system used in the stripping voltammetry mathematical model, and the experimental and simulated voltammetry for the reverse scan CVs of $AgNTf_2$ and $AgNO_3$. This material is available free of charge via the Internet at http://pubs.acs.org.

References and Notes

(1) Silvester, D. S.; Compton, R. G. *Z. Phys. Chem.* **2006**, *220*, 1247.
(2) Buzzeo, M. C.; Evans, R. G.; Compton, R. G. *ChemPhysChem* **2004**, *5*, 1106.
(3) Endres, F.; Zein El Abedin, S. *PhysChemChemPhys* **2006**, *8*, 2101.
(4) Hultgren, V. M.; Mariotti, A. W. A.; Bond, A. M.; Wedd, A. G. *Anal. Chem.* **2002**, *74*, 3151.
(5) Saheb, A.; Janata, J.; Josowicz, M. *Electroanalysis* **2006**, *18*, 405.
(6) Ohno, H. *Electrochemical Aspects of Ionic Liquids*; J. Wiley and Sons Inc.: Hoboken, NJ, 2005.
(7) Silvester, D. S.; Rogers, E. I.; Compton, R. G. In Reference Electrodes for Use in RTILs. *Electrodeposition in Ionic Liquids*; Endres, F., MacFarlane, D., Abbot, A., Eds.; Wiley-Interscience: New York, 2007; Chapter 13.2.
(8) Butler, J. N. *Reference Electrodes in Aprotic Organic Solvents*; Wiley Interscience: New York, 1970.
(9) Ives, D. J. G.; Janz, G. J. *Reference Electrodes: Theory and Practice;* Academic Press: New York, 1961.
(10) Reiger, P. H. *Electrochemistry*, 2nd ed.; Chapman and Hall: New York 1994.
(11) Grutzner, G.; Kuta, J. *Pure Appl. Chem.* **1984**, *56*, 461.
(12) Snook, G. A.; Best, A. S.; Pandolfa, A. G.; Hollenkamp, A. F. *Electrochem. Commun.* **2006**, *8*, 1405.
(13) Fietkau, N.; Clegg, A. D.; Evans, R. G.; Villigrán, C.; Hardacre, C.; Compton, R. G. *ChemPhysChem* **2006**, *7*, 1041.
(14) MacFarlane, D. R.; Meakin, P.; Sun, J.; Amini, N.; Forsyth, M. J. *J. Phys. Chem. B* **1999**, *103*, 4164.
(15) Michaelis, L.; Granick, S. *J. Am. Chem. Soc.* **1943**, *65*, 1747.
(16) Yamauchi, J.; Fujita, H.; Deguchi, Y. *Bull. Chem. Soc. Jpn.* **1979**, *52*, 2819.
(17) Note that the purpose of our work is the measurement of electrode kinetics not formal potentials. Accordingly, the use of quasi-reference electrodes does not compromise the values of k^0 extracted, provided it remains stable on the experimental voltammetric time scale.
(18) Silvester, D. S.; Wain, A. J.; Aldous, L.; Hardacre, C.; Compton, R. G. *J. Electroanal. Chem.* **2006**, *596*, 131. Schröder, U.; Wadhawan, J. D.; Compton, R. G.; Marken, F.; Suarez, P. A. Z.; Consorti, C. S.; de Souza, R. F.; Dupont, J. *New J. Chem.* **2000**, *24*, 1009.
(19) Sharp, M. *Electrochim. Acta* **1983**, *28*, 301.
(20) Shoup, D.; Szabo, A. *J. Electroanal. Chem.* **1982**, *140*, 237.
(21) Evans, R. G.; Klymenko, O. V.; Saddoughi, S. A.; Hardacre, C.; Compton, R. G. *J. Phys. Chem. B* **2004**, *108*, 7878.
(22) Strikwerda, J. C. *Finite Difference Schemes and Partial Differential Equations*; Wadsworth & Brookes: Pacific Grove, CA, 1989.
(23) Arfken, G. B.; Weber, H. J. *Mathematical Methods for Physicists*; Academic Press: San Diego, CA, 2001.
(24) Fisher, A. C.; Compton, R. G. *J. Phys. Chem.* **1991**, *95*, 7538.
(25) Gavaghan, D. J. *J. Electroanal. Chem.* **1998**, *456*, 1.
(26) Note: This was the most stable reference electrode available at the present time.
(27) Aldous, L.; Silvester, D. S.; Villagrán, C.; Pitner, W. R.; Compton, R. G.; Hardacre, C. *New J. Chem.* **2006**, *30*, 1576.
(28) Silvester, D. S.; Aldous, L.; Lagunas, M. C.; Hardacre, C.; Compton, R. G. *J. Phys. Chem. B* **2006**, *110*, 22035.
(29) He, P.; Liu, H.; Li, Z.; Liu, Y.; Xu, X.; Li, J. *Langmuir* **2004**, *20*, 10260.
(30) Evans, R. G.; Klymenko, O. V.; Hardacre, C.; Seddon, K. R.; Compton, R. G. *J. Electroanal. Chem.* **2003**, *556*, 179.
(31) Sudha, V.; Sangaranarayanan, M. V. *J. Chem. Sci.* **2005**, *117*, 207.
(32) Simm, A. O.; Banks, C. E.; Ward-Jones, S.; Davies, T. J.; Lawrence, N. S.; Jones, T. G. J.; Jiang, L.; Compton, R. G. *Analyst* **2005**, *130*, 1303.
(33) Harned, H. S.; Hildreth, C. L. *J. Am. Chem. Soc.* **1951**, *73*, 3292.
(34) Nakagawa, S.; Takehara, Z.; Yoshizawa, S. *Electrochim. Acta* **1973**, *18*, 1043.
(35) "In-house" value obtained from this particular ionic liquid.
(36) www.princetonappliedresearch.com (accessed March, 2007).
(37) Evans, R. G.; Klymenko, O. V.; Price, P. D.; Davies, S. G.; Hardacre, C.; Compton, R. G. *ChemPhysChem* **2005**, *6*, 526.
(38) Rudolph, M.; Reddy, D. P.; Feldberg, S. W. *Anal. Chem.* **1994**, *66*, 589A.
(39) Bard, A. J.; Faulkner, L. R. *Electrochemical Methods: Fundamentals and Applications*, 2nd ed.; Wiley: New York, 2001.
(40) Alden, J. A.; Hutchinson, F.; Compton, R. G. *J. Phys. Chem. B* **1997**, *101*, 949.